

Gas-phase mass-transfer resistance at PEMFC electrodes Part 2. Effects of the flow geometry and the related pressure field

E. Arato*, M. Pinna, P. Costa

Department of Environmental Engineering-DIAM, University of Genoa, Via Opera Pia 15, 16145 Genoa, Italy

Received 15 July 2005; received in revised form 12 January 2006; accepted 13 January 2006

Available online 24 February 2006

Abstract

It has been demonstrated that it is possible to have a better understanding of the mass-transfer phenomena occurring at PEMFC electrodes by distinguishing the various diffusive regimes taking place inside the porous layer close to the electrodes themselves. In each regime the interactions between diffusive and forced flows have been expressed in terms of Peclet numbers and the overall diffusive resistances have been expressed in terms of Sherwood numbers.

Now the comparison of traditional and non-traditional geometrical arrangements can be more fully discussed and the geometrical optimisation of the cell can be more clearly determined by explicitly considering the role of the geometrical arrangement of the cell channels and the related pressure field.

Both interdigitated and serpentine cells can be operated in such a way that high Sherwood numbers and, then, a high limit current are attained. Both types of cells are penalised by higher head losses than traditional cells, but these appear to be much greater in the serpentine arrangement.

The ultimate goal of reaching high, almost uniform Sherwood numbers and low head losses is still problematic. A partially interdigitated configuration might be a step in the right direction.

© 2006 Elsevier B.V. All rights reserved.

Keywords: Transport phenomena; Modelling; Polymeric membrane fuel cells; Gas flow mode

1. Introduction

In the first part of this work [1] attention was focused on the gas-phase mass transfer occurring at PEMFC electrodes. The various possible diffusive regimes were determined for each regime, the interaction between diffusive and forced flows was expressed in terms of the Peclet number and then, the overall diffusive resistance was expressed in terms of the Sherwood numbers as a function of the Peclet numbers.

The results of this approach have been used in the discussion of a number of experimental findings relating to traditional [2,3], interdigitated [4–7] and serpentine [8] cells. A better understanding of the role of the gas mass transfer has been shown to be effective in explaining some important differences in the performance of these cells, especially in terms of limit current.

Now, in the second part of this work the comparison of interdigitated and serpentine geometries will be further developed by explicitly taking into account the pressure differences between contiguous channels and their dependence on the head losses through the channels. These results are currently available as the output of detailed cell models [7,9]; here, a simplified, analytical solution is proposed, by means of which the differences between different geometrical arrangements can be immediately appreciated.

Both interdigitated and serpentine cells can be operated at high Sherwood numbers corresponding to high limit currents [1,9], but both are correspondingly penalised by higher head losses than traditional cells, this being much greater in the case of the serpentine arrangement. A better understanding of these features will allow us to more effectively plan the geometrical optimisation of the cell.

However, the ultimate goal of reaching high and uniform Sherwood numbers in all parts of the cell plane and low head losses is still problematic, and even interdigitated cells do not

* Corresponding author. Tel.: +39 010 3532926; fax: +39 010 3532589.
E-mail address: beta@diam.unige.it (E. Arato).

Nomenclature

A	relative permeability—def. (4)
b	width of a channel (m)
B	def. (19)
c	characteristic velocity of Eq. (42) (m s^{-1})
C_1, C_2, C_3, C_4	integration constants—def. (10)
C_5, C_6, C_7, C_8	integration constants—def. (23)
d	length of the diffusive layer (m)
d_f	diameter of the holes interconnecting the channels (m)
D	effective diffusivity in the porous medium ($\text{m}^2 \text{s}^{-1}$)
D_M	molecular diffusivity in the continuous gas phase ($\text{m}^2 \text{s}^{-1}$)
f_c, f_f, f_p, f_s	shape factors
h	thickness of the diffusive layer (m)
k	permeability of the porous medium (m^2)
L	length of the channel (m)
M	def. (44)
n_c	number of channels in a cell
N	mass flux ($\text{kg m}^{-2} \text{s}^{-1}$)
p	dimensionless pressure
P	absolute pressure ($\text{kg m}^{-1} \text{s}^{-2}$)
P_r	reference pressure—def. (4) ($\text{kg m}^{-1} \text{s}^{-2}$)
Pe_x	transversal Peclet number
Pe_y	axial Peclet number
Sh	Sherwood number
u	velocity in the channel (m s^{-1})
u_r	inlet (maximum) u velocity (m s^{-1})
v	velocity in the porous medium (m s^{-1})
v_r	reference velocity for v —def. (4) (m s^{-1})
x	spatial coordinate, perpendicular to the electrode (m)
y	spatial coordinate, parallel to the electrode (m)
z	dimensionless spatial coordinate along the channel
Z	spatial coordinate, parallel to the channel (m)

Greek letters

Δ	dimensionless head loss—def. (19)
φ	interdigitation degree
μ	viscosity of the gas ($\text{kg m}^{-1} \text{s}^{-1}$)
ρ	density of the gas (kg m^{-3})

Superscripts and subscripts

c	channel
f	interconnecting hole
L	end of the channel
p	permeable boundary
r	reference value
s	porous medium
0	beginning of the channel
$0, 1, 2, 3$	four successive channels
'	refers to serpentine arrangement

seem to be able to supply a completely satisfactory answer to this problem at present. The partially interdigitated configuration proposed in the final section of this work might be a step in the right direction.

Reference schemes for the geometrical arrangements for an interdigitated (Fig. 1a) and a serpentine (Fig. 1b) configuration, respectively, considered are reported in Fig. 1.

2. The flow field for interdigitated geometry

As discussed in the first part of this work [1], a good estimation of the velocity of migration in the porous medium close to the electrode is an important and necessary premise for a good estimation of the Sherwood number and, then, the limit current. The well-known integrated one-dimensional permeability equation

$$v = \frac{f_s k (P_1 - P_2)}{\mu d} \quad (1)$$

is probably accurate enough to evaluate the velocity of migration when $(P_1 - P_2) \ll P_1$ and a substantially one-dimensional migration path ($h \ll d$; see Fig. 1, Part 1 of this work [1]), but it requires a knowledge of the driving force $(P_1 - P_2)$ and this,

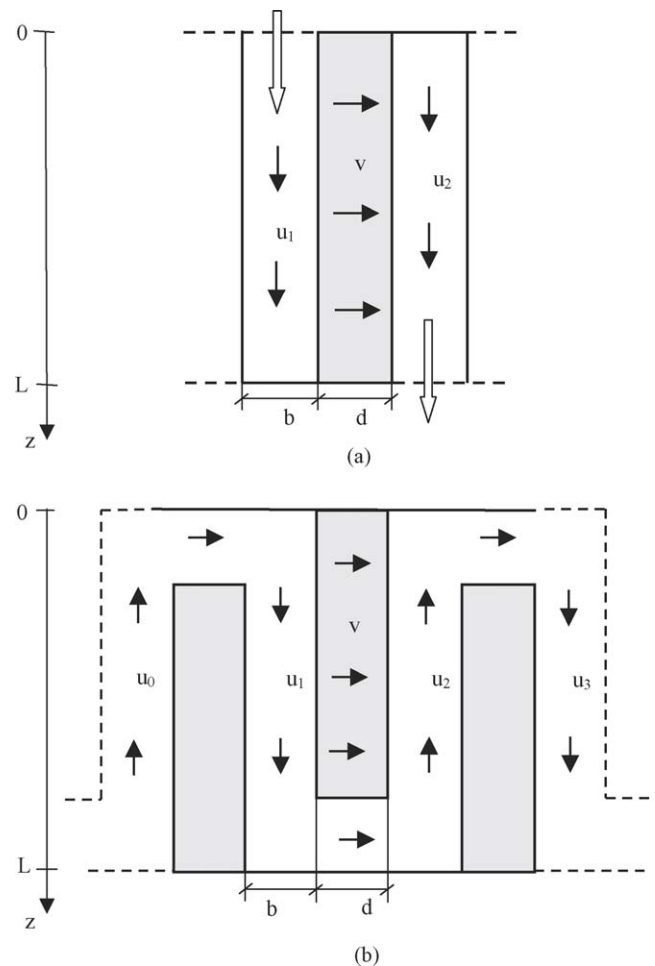


Fig. 1. Reference geometrical and flow schemes for an electrode element: (a) an interdigitated arrangement and (b) a serpentine arrangement.

in turn, depends on the head losses inside the channels and the channel mass balance.

Eq. (1) and the consequent evaluation of the local Sherwood number can be included in a detailed simulation tool, so that the effects of the gas mass transfer towards the electrodes is more correctly taken into account and a better prediction of the cell's behaviour at high currents can be obtained. Some examples of the results obtainable using this method have been reported in the first part of this work. Here, simplified analytical solutions for the flow and pressure fields are presented, so that the differences between the various geometrical arrangements can be fully demonstrated.

With reference to a pair of interdigitated channels, 1 and 2, under the simplified condition of constant total flow rate, the mass and momentum balances can be written

$$\frac{dP_1}{dZ} = -\frac{f_c 32 u_1 \mu}{b^2}, \quad \frac{dP_2}{dZ} = -\frac{f_c 32 u_2 \mu}{b^2} \quad (2)$$

$$\frac{du_1}{dZ} = -\frac{f_p v h}{b^2}, \quad \frac{du_2}{dZ} = +\frac{f_p v h}{b^2} \quad (3)$$

where each channel is assumed to be in a laminar regime and the migration flow rate lost by the first channel is acquired by the second.

The constant volumetric flow rate assumption (in synthesis $u_1 + u_2 = \text{constant}$) needs some further explanation. Strictly speaking, it should correspond to the assumption of null current, because the electrochemical reaction necessarily implies a flow rate variation, a decrease at the anode and an increase at the cathode. Moreover, any temperature distribution in the cell is associated with further volumetric flow rate changes. Bearing in mind these considerations, the reference to a mean, constant, volumetric flow rate could seem an oversimplification. On the other hand, the pressure drops to be considered are, primarily, those taking place at the cathode, where the molar flow rate variations of the supplied air are of the order of a 4–6%, so that the assumption of a mean flow rate value implies quite acceptable uncertainties (less than 3%). Errors on the anodic side could be significantly greater (namely 30–40%), but the problem of the anodic pressure drops is significantly less important. However, if one is interested in a more exact evaluation of the flow field on both sides, taking effective flow rate changes as well as temperature distributions into account, detailed cell models are available [7,9]. The simplified approach used here offers the advantage of an explicit analytical solution that is easily suited to a substantially quantitative discussion of different cell arrangements.

By combining Eqs. (1)–(3) and by defining the dimensionless parameters and variables

$$v_r = \frac{u_r b^2}{f_p h L}, \quad P_r = \frac{f_c 32 u_r \mu L}{b^2},$$

$$A^2 = \frac{f_c f_p f_s 64 k h L^2}{d b^4} \quad (4)$$

$$p = \frac{P}{P_r}, \quad z = \frac{Z}{L} \quad (5)$$

the following system of differential equations is obtained:

$$\frac{d^2(p_1 - p_2)}{dz^2} = A^2(p_1 - p_2), \quad \frac{d^2(p_1 + p_2)}{dz^2} = 0 \quad (6)$$

For an interdigitated geometry the boundary conditions to be added to the equations in (6) are

$$z = 0; \quad u_1 = u_r; \quad u_2 = 0, \quad \frac{dp_1}{dz} = -1,$$

$$\frac{dp_2}{dz} = 0, \quad \frac{d(p_1 - p_2)}{dz} = -1 \quad (7)$$

$$z = 1; \quad u_1 = 0; \quad u_2 = u_r, \quad \frac{dp_1}{dz} = 0,$$

$$\frac{dp_2}{dz} = -1, \quad \frac{d(p_1 - p_2)}{dz} = 1 \quad (8)$$

The solution

$$p_1 - p_2 = C_1 \exp(Az) + C_2 \exp(-Az),$$

$$p_1 + p_2 = C_3 z + C_4 \quad (9)$$

with

$$C_1 = \left(\frac{1}{A}\right) \left[\frac{1 + \exp(-A)}{\exp(A) - \exp(-A)} \right]$$

$$C_2 = \left(\frac{1}{A}\right) \left[\frac{1 + \exp(A)}{\exp(A) - \exp(-A)} \right] \quad (10)$$

$$C_3 = -1$$

demonstrates that the migration velocities v , which are proportional to the pressure difference,

$$\frac{v}{v_r} = \left(\frac{A^2}{2}\right) (p_1 - p_2), \quad v_m = v_r \quad (11)$$

are symmetrical to the middle of the cell ($z = 1/2$), while the velocities along the channels, which are proportional to the pressure derivatives, are anti-symmetrical. The overall head losses for the pair of interdigitated channels is

$$p_{10} - p_{2L} = \frac{C_1[1 + \exp(A)] + C_2[1 + \exp(-A)] + 1}{2} \quad (12)$$

and the fraction of the entire flow rate that migrates through the porous medium from the first channel to the second (by pass fraction) corresponds, obviously, to unity ($v_m/v_r = 1$).

The main parameter determining the flow field configuration is A , which is a function of the permeability of the porous medium and the geometry of the system. The effects of parameter A on the flow fields and the pressure field in an interdigitated arrangement are illustrated in Fig. 2.

By varying A the following limit cases can be considered. When the permeability is much higher than the head losses of the channels

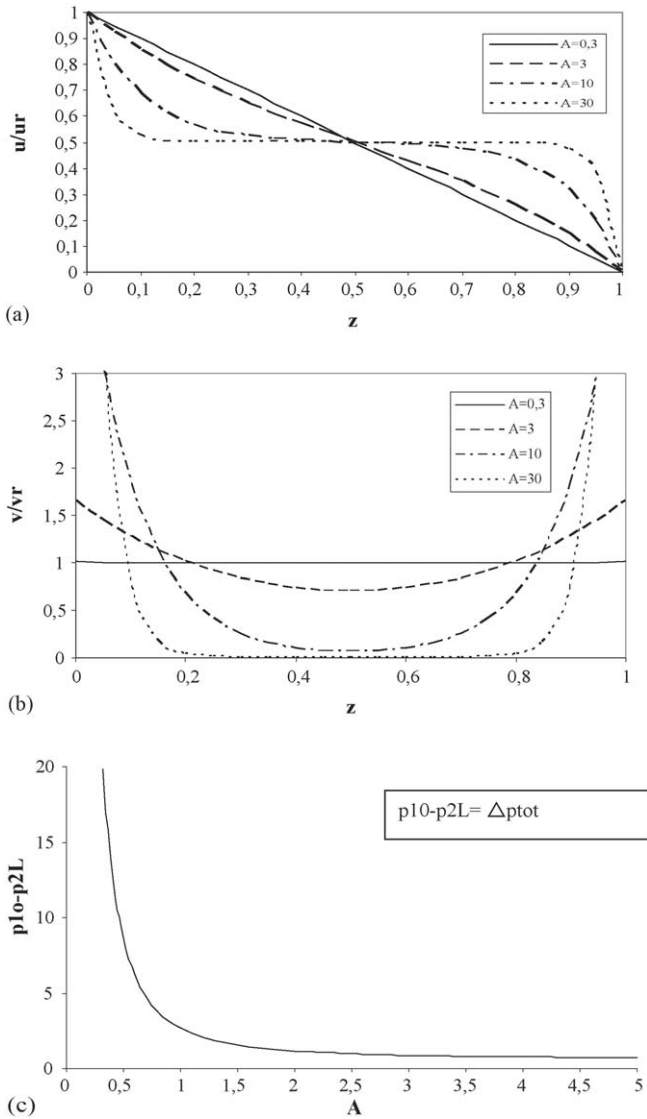


Fig. 2. The distribution of the flow rate between two adjacent interdigitated channels along the axial coordinate for various values of parameter A : (a) the velocity inside the first channel (u/u_r) and (b) the migration velocity between channels (v/v_r). (c) The trend of the global head losses ($p_{10} - p_{2L}$) as a function of parameter A .

• $A \gg 1$

$$\frac{u_1}{u_r} \approx \frac{1 + \exp(-Az) - \exp(-A + Az)}{2} \quad (13)$$

$$\frac{v}{v_r} \approx \left(\frac{A}{2}\right) [\exp(-Az) + \exp(-A + Az)]$$

$$p_{10} - p_{2L} \approx \frac{1}{2} \quad (14)$$

half of the entire flow rate is almost immediately transferred from one channel to the other, then each channel conveys half the flow rate, with overall head losses almost equal to a half of the ones pertinent to a single channel with a velocity u_r (or equal to the ones pertinent to a single channel with a velocity $u_r/2$). The remaining half flow rate is transferred to the second channel immediately before the exit point.

Obviously, a pair of interdigitated channels does not operate in this way. The correct operating conditions are, on the contrary, nearer to the second limit case, where the permeability of the porous medium is low.

• $A \ll 1$

$$\frac{u_1}{u_r} \approx 1 - z, \quad \frac{v}{v_r} \approx 1 \quad (15)$$

$$p_{10} - p_{2L} \approx \frac{2}{A^2} \gg 1 \quad (16)$$

and the overall head losses are controlled by this low permeability and are much greater than the ones of a single channel. In this case, the velocity of migration v is almost uniform along the entire channel length (z axis).

As an effective interdigitation should require $A < 1$, the global head losses of the cell are correspondently high (see Fig. 2c). A good compromise can be reached by choosing values of A of the order of 3, so that a good distribution of the interdigitation flow is achieved in correspondence to the global head losses that are only a little greater than those of the traditional arrangement.

3. The flow field for serpentine geometry

The serpentine geometry, also in its simplest, single channel version, is a little more difficult to analyse than the interdigitated one. The study of two contiguous channels (1 and 2), now with countercurrent velocities, needs to consider another two, external, channels (0 and 3), which are also involved in an exchange of mass with the preceding. On the other hand, the simplification of the repeatable trend of the head losses along the serpentine channel can be introduced

$$p_0(z) = p_2(z) + 2\Delta, \quad p_3(z) = p_1(z) - 2\Delta \quad (17)$$

and, then a formulation strictly similar to (6) can be attained

$$\frac{d^2(p_1 - p_2 - \Delta)}{dz^2} = B^2(p_1 - p_2 - \Delta),$$

$$s \frac{d^2(p_1 + p_2)}{dz^2} = 0 \quad (18)$$

$$B^2 = 2A^2, \quad 2\Delta = p_{0L} - p_{1L} = p_{2L} - p_{3L} = p_{10} - p_{20} \quad (19)$$

On the other hand, the correct set of boundary conditions is now

$$z = 0; \quad u_2 = -u_1, \quad p_1 - p_2 = 2\Delta,$$

$$\frac{d(p_1 + p_2)}{dz} = 0 \quad (20)$$

$$z = 1; \quad u_2 = -u_1, \quad p_1 - p_2 = 0, \quad \frac{d(p_1 + p_2)}{dz} = 0 \quad (21)$$

so that the solution

$$\begin{aligned} p_1 - p_2 &= C_5 \exp(Bz) + C_6 \exp(-Bz) + \Delta, \\ p_1 + p_2 &= C_7 z + C_8 \end{aligned} \quad (22)$$

$$\begin{aligned} C_5 &= -\frac{\Delta[1 + \exp(-B)]}{\exp(B) - \exp(-B)} \\ C_6 &= \frac{\Delta[1 + \exp(B)]}{\exp(B) - \exp(-B)} \\ C_7 &= 0 \end{aligned} \quad (23)$$

demonstrates that this time u is symmetrical and v anti-symmetrical to the middle of the cell:

$$\begin{aligned} \frac{u_1}{u_r} &= -\frac{dp_1}{dz} = -\left(\frac{1}{2}\right) \frac{d(p_1 - p_2)}{dz} \\ &= \left(\frac{\Delta B}{2}\right) \frac{[1 + \exp(-B)] \exp(Bz) + [1 + \exp(B)] \exp(-Bz)}{\exp(B) - \exp(-B)} \end{aligned} \quad (24)$$

c

$$\frac{v}{v_r} = \left(\frac{B^2}{4}\right) (p_1 - p_2), \quad v_m < v_r \quad (25)$$

The by-pass fraction, corresponding to the mean value of v , is now

$$\frac{v_m}{v_r} = \left(\frac{B^2}{4}\right) (p_1 - p_2)_m = \left(\frac{B^2}{4}\right) \Delta \quad (26)$$

and the sum of (24) and (26) corresponds to unity, that is it represents the whole reference flow rate through the cell. This last condition makes it possible to evaluate the head loss parameter

$$\Delta = \left\{ \left(\frac{B^2}{4}\right) + \frac{B}{2} \left[\frac{\exp(B) + \exp(-B) + 2}{\exp(B) - \exp(-B)} \right] \right\}^{-1} \quad (27)$$

The effects of parameter A on the flow fields and the pressure field in a serpentine arrangement are illustrated in Fig. 3.

With regard to the limit cases, when the permeability is high

• $B \gg 1$

$$\Delta \approx \frac{4}{B^2}, \quad v_m \approx v_r \quad (28)$$

$$\begin{aligned} \frac{u_1}{u_r} &\approx \left(\frac{2}{B}\right) [\exp(-Bz) + \exp(-B + Bz)] \\ \frac{v}{v_r} &\approx 1 + \exp(-Bz) - \exp(-B + Bz) \end{aligned} \quad (29)$$

almost the entire flow rate is transferred through the porous layer (the by-pass fraction is only a little less than unity), while the velocity along most of the channels and the corresponding flow rate fraction are very low.

This first limit case may seem interesting, but it is not very realistic: even in the serpentine geometry the most likely limit case is the one corresponding to low permeability.

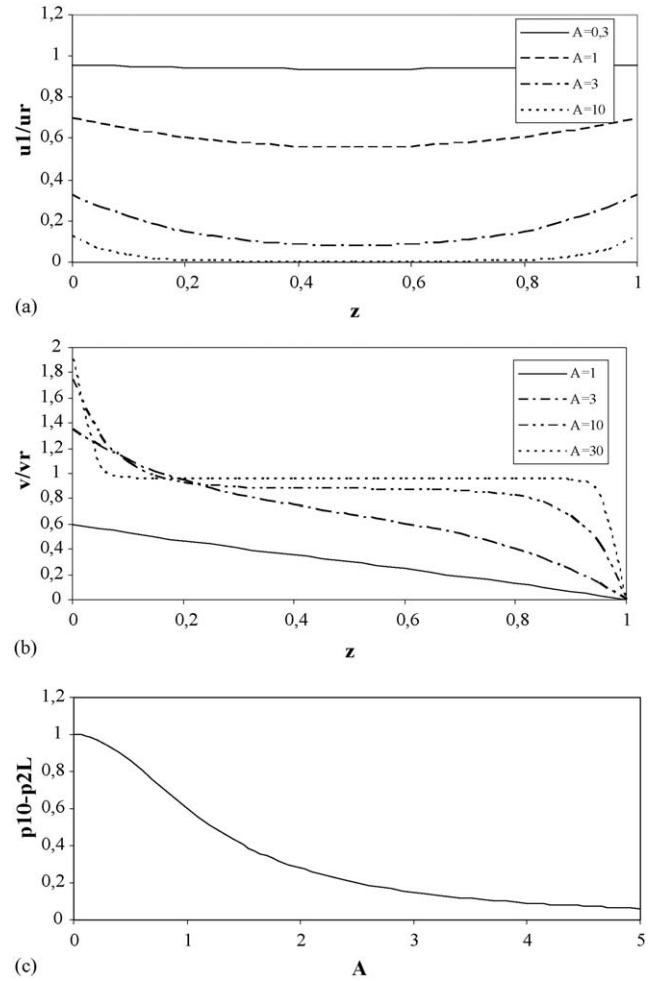


Fig. 3. The distribution of the flow rate between two adjacent serpentine channels along the axial coordinate for various values of parameter A ($A^2 = B^2/2$): (a) the velocity inside the first channel (u/u_r) and (b) the migration velocity between channels (v/v_r). (c) The trend of the global head losses ($p_{10} - p_{20}$) as a function of parameter A .

• $B \ll 1$

$$\Delta \approx 1, \quad \frac{v_m}{v_r} \approx \frac{B^2}{4} \ll 1 \quad (30)$$

$$\frac{u_1}{u_r} \approx 1, \quad \frac{v}{v_r} \approx \left(\frac{B^2}{2}\right) (1 - z) \ll 1 \quad (31)$$

which controls the overall head losses. In this case, the velocity of migration v is very low and strongly asymmetrical, while the head losses of the channel are only slightly affected by the very low by-pass fraction.

In a serpentine cell the single channel head losses are higher than in the traditional arrangement because the velocity is higher; the decrease corresponding to the increase in the by-pass fraction (see Fig. 3c) is not decisive; moreover, the global head losses depend on the number of passages, so that increasing the cell size quickly makes them unacceptable.

4. The order of magnitude of the parameters

We can assume unit values for the various shape factors and we have referred to literature values for the geometrical and physical parameters:

$$h = 2 \times 10^{-2} \text{ cm}, \quad L = 10 \text{ cm}, \quad d = b = 10^{-1} \text{ cm}$$

$$k = 10^{-8} \text{ cm}^2, \quad \mu = 10^{-4} \text{ g cm}^{-1} \text{ s}^{-1},$$

$$s\Delta P_r = 3 \times 10^3 \text{ Pa} = 3 \times 10^4 \text{ g cm}^{-1} \text{ s}^{-2}$$

$$D_M = 0.2 \text{ cm}^2 \text{ s}^{-1}, \quad \frac{D}{D_M} = 0.1$$

and we have also defined [1]

the axial Peclet number: $Pe_y = dv/D$

the transversal Peclet number: $Pe_x = h^2v/dD$

and the Sherwood number Sh as the ratio between the actual mean flux of the electrochemical reagent and a reference flux [1].

Then, by making these assumptions the transition from the diffusive to the forced regime can be situated around $Pe_y = 25$ and the transition from the forced flow rate to the forced pellicular regime around $Pe_y = 60$. Moreover, the above set of data leads to

$$A^2 = 0.13, \quad A = 0.35, \quad B = 0.5$$

so that such approximations as $\exp(A) \approx 1 + A$ are correct to within a few percent and, then, a sure reference can be made to the limit cases of low permeability. However, it should be kept in mind that a relatively little change in the geometrical or physical parameters is also sufficient to make this simplification less accurate and raise the values of B to the order of unity.

For the interdigitated geometry, with $A = 0.35$, the velocity of migration and the corresponding Peclet numbers are

$$v = 30 \text{ cm s}^{-1}, \quad Pe_y = 150, \quad Pe_x = 6, \quad Sh = 0.9$$

So, the migration through the porous medium takes place under a forced regime and, prevalently, under a forced pellicular regime. Under such conditions the Sherwood number is of the order of unity.

For the serpentine geometry, with $B = 0.5$, the velocities of migration are undoubtedly lower; a mean value is about

$$v = 2 \text{ cm s}^{-1}, \quad Pe_y = 10, \quad Pe_x = 0.4, \quad Sh = 0.3$$

so that the migration still takes place in a substantially diffusive regime, with Sherwood numbers of the order of 0.3.

A significant increase in the velocity of migration and the Sherwood number can only occur when the head losses are strongly increased, as is clearly demonstrated by the results reported by Zhukovsky and Pozio [8].

Another way of looking at the question, so that the different flow conditions of a serpentine channel and an interdigitated configuration can more clearly be taken into account, is to consider the by-pass fractions and the overall head losses in the two

cases. Assuming low permeability regimes ($A \ll 1$; $B \ll 1$), the interdigitated case is characterised by

$$v = v_r = \frac{u_r b^2}{f_p h L}, \quad |\Delta P| = \frac{2P_r}{A^2} = \frac{f_c 64 u_r \mu L}{A^2 b^2}$$

while the serpentine is characterised by

$$v_m = \frac{B^2 v_r}{4} = \frac{B^2 u_r' b^2}{f_p h L}, \quad |\Delta P| = \frac{f_c 32 u_r' \mu L'}{b^2}$$

Under the same cell flow rate and the same number of channels for the cell,

$$u_r' = \frac{u_r n_c}{2}, \quad L' = L n_c$$

the comparison of the by-pass fractions

$$\frac{(v_m)_{\text{serp}}}{v_{\text{interd}}} = \frac{B^2 n_c}{8} = \frac{A^2 n_c}{4} \quad (32)$$

even when not considering the highly asymmetrical distribution of the serpentine, strongly favours the interdigitated geometry, unless the number of channels is very high. But in such a case the comparison of the head losses

$$\frac{|\Delta P|_{\text{serp}}}{|\Delta P|_{\text{interd}}} = \frac{A^2 n_c^2}{4} \quad (33)$$

should demonstrate that the overall serpentine head losses are much greater than the already considerable ones that characterise an interdigitated cell.

5. The partial interdigitated geometry

In the preceding section, we demonstrated how the serpentine geometry could contribute to lowering the diffusive resistances only if heavy overall head losses are allowed. On the other hand, Zhukovsky and Pozio have underlined how a significant lowering of the diffusive resistances can also be attained by using geometries that are characterised by rather moderate migration velocities.

The interdigitated geometries also have greater head losses than the traditional geometries but, on the other hand, they permit migration velocities that are often greater than what is needed. For instance, if the migration velocity of the above example were of 20 cm s^{-1} instead of 30 cm s^{-1} , we would still have $Pe_y = 100$, a forced flow rate regime and $Sh = 0.6$, sufficient for a significant increase in the limit current.

A useful modification to the interdigitated geometry is what could be referred to as “partially interdigitated”: instead of feeding the entire flow rate of a pair of channels only to the first channel, so that it transversally migrates to the second and exits entirely from that one, one could feed a fraction $(1 + \varphi)/2$ of the flow rate to the first channel and a fraction $(1 - \varphi)/2$ to the second, so that only the fraction φ (interdigitation degree) is forced to migrate transversally from one channel to the other and, at the exit, the first channel still conveys the fraction $(1 - \varphi)/2$ to the exit and the second the fraction $(1 + \varphi)/2$. The correct distribution of the flow rate in the two channels could be obtained by means of calibrated holes and (low) localised head losses.

The differential equations in (6) are still valid for this partial interdigitated geometry, but the boundary conditions have to be changed in order to allow for the different distribution of the flow rate

$$z = 0, \quad \frac{dp_1}{dz} = -\frac{1+\varphi}{2}, \quad \frac{dp_2}{dz} = -\frac{1-\varphi}{2},$$

$$\frac{d(p_1 - p_2)}{dz} = -\varphi \quad (34)$$

$$z = 1, \quad \frac{dp_1}{dz} = -\frac{1-\varphi}{2}, \quad \frac{dp_2}{dz} = -\frac{1+\varphi}{2},$$

$$\frac{d(p_1 - p_2)}{dz} = \varphi \quad (35)$$

A solution such as (9) is still obtained, with the integration constants C_1 and C_2 multiplied by a factor φ over the values in (10) and, again, $C_3 = -1$. The velocities of migration through the porous layer, which are still symmetrical, are reduced by the factor φ

$$\frac{v}{v_r} = \left(\frac{\varphi A^2}{2}\right) (p_1 - p_2), \quad v_m = \varphi v_r \quad (36)$$

just as the overall head losses of the two channels are similarly reduced

$$p_{10} - p_{2L} = \left(\frac{\varphi}{A}\right) \frac{[1 + \exp(A)][1 + \exp(-A)]}{\exp(A) - \exp(-A)} + \frac{1}{2} \quad (37)$$

The by-pass fraction obviously corresponds to the interdigitation degree ($v_m/v_r = \varphi$). In particular, the low permeability limit case now predicts

- $A \ll 1$

$$\frac{u_1}{u_r} \approx \frac{1 + \varphi - 2\varphi z}{2}, \quad \frac{v}{v_r} \approx \varphi \quad (38)$$

$$p_{10} - p_{2L} \approx \frac{2\varphi}{A^2} \quad (39)$$

so that the overall head losses can be significantly reduced without hampering the limit current too much.

The partially interdigitated geometry could present a further advantage. As has already been said, partial interdigitation can be realised by means of calibrated holes that connect a pair of channels at their beginning and at their end so that the flow rate distribution between the two depends on the localised head losses of the holes

$$(P_1 - P_2)_0 = (P_1 - P_2)_L = \left(\frac{\rho f_f}{2}\right) \left[u_r \left(\frac{b}{d_f}\right)^2 (1 - \varphi) \right]^2 \quad (40)$$

Recalling Eq. (1) and making reference to low permeability ($A \ll 1$), so that $(P_1 - P_2)_0 = (P_1 - P_2)_L = P_1 - P_2 = \Delta P$ and $v(z) = \text{constant}$, we have

$$v = \varphi \left(\frac{u_r b^2}{hd}\right) = \frac{f_s k \Delta P}{\mu d} \quad (41)$$

and the following equation in φ can be written:

$$\varphi = \frac{(1 - \varphi^2) u_r}{c}, \quad c = \frac{2\mu d d_f^4}{f_f \rho k l b^2} \quad (42)$$

The interdigitation degree

$$\varphi = \frac{-1 + [1 + 4(u_r/c)^2]^{1/2}}{2u_r/c} \quad (43)$$

is then an increasing function of the velocity u_r . In turn, the migration velocity

$$v = M \varphi u_r, \quad M = \frac{b^2}{hd} \quad (44)$$

shows a more than linear increase with u_r , that is the whole flow rate of the two channels. So, when the desired current, and then the flow rate, is increased, the utilisation degree being equal, the partially interdigitated cell responds with an increase in the interdigitation degree and a more effective increase in the migration velocity, the Sherwood number and the limit current, at the expense of a lower increase in the overall head losses.

Acknowledgment

This work has been partially supported by the Italian National Agency for New Technologies, Energy and the Environment (ENEA) within the framework of the FISIR 2003 financed research project.

References

- [1] E. Arato, P. Costa, J. Power Sources, in press.
- [2] S.-H. Ge, B.-L. Yi, J. Power Sources 124 (2003) 1.
- [3] P. Costamagna, Chem. Eng. Sci. 56 (2001) 323.
- [4] T.F. Fuller, J. Newman, J. Electrochem. Soc. 140 (1993) 1218.
- [5] U. Sukkee, C.Y. Wang, J. Power Sources 125 (2004) 40.
- [6] D.L. Wood III, Jung S. Yi, T. Van Nguyen, Electrochim. Acta 24 (1998) 3795.
- [7] A. Serrafiero, E. Arato, P. Costa, J. Power Sources 145 (2) (2005) 470.
- [8] K. Zhukovsky, A. Pozio, J. Power Sources 130 (2004) 95.
- [9] A. Serrafiero, E. Arato, P. Costa, Proc. H2 age: When, Where, Why (Pisa, Italy, May 2004), Chem. Eng. Trans. 4 (2004) 423 (Edit. Sauro Pierucci, AIDIC Servizi S.r.l., Milano).